Multiple Regions of Subunit Interaction in *Drosophila* Mitochondrial DNA Polymerase: Three Functional Domains in the Accessory Subunit†

Li Fan and Laurie S. Kaguni*

Department of Biochemistry and Molecular Biology, Michigan State University, East Lansing, Michigan 48824-1319

Received January 16, 2001

ABSTRACT: *Drosophila* mitochondrial DNA polymerase, pol γ, is a heterodimeric complex of catalytic subunit and accessory subunits. Physical interactions between the two subunits were investigated by deletion mutagenesis in both in vivo reconstitution and in vitro protein overlay analyses. Our results suggest that the accessory subunit may consist of three domains, designated the N, M, and C domains. The M and C regions comprise the major contacts involved in subunit interaction, likely with multiple sites in the exonuclease (exo) region and part of the spacer between the exo and DNA polymerase (pol) regions in the catalytic subunit. Furthermore, the N region in the accessory subunit may modulate subunit assembly and/or conformation through weak interaction with the pol region in the catalytic subunit. Sequence comparisons identify a significant similarity between the M region of the accessory subunit and the RNase H domain of HIV-1 reverse transcriptase. On the basis of these results, the proposed function of the C-terminus of the accessory subunit in RNA primer recognition, and previous observations that mitochondrial DNA polymerase is itself a reverse transcriptase, we propose that the overall conformation and arrangement of functional regions in the *Drosophila* pol γ complex resemble those of HIV-1 reverse transcriptase.

Drosophila mitochondrial DNA polymerase, typical of animal pol γs,[1] is a processive, highly faithful and salt-stimulated replicative DNA polymerase which catalyzes DNA synthesis on a variety of template-primer substrates including poly(rA):oligo(dT) (*1*, *2*). Also typical of animal pol γs, the *Drosophila* enzyme is a heterodimer of catalytic and accessory subunits (*1*, *3*) that are encoded by nuclear genes (*4*, *5*). The catalytic subunit, pol $\gamma-\alpha$, contains both DNA polymerase and 3′-5′ exonuclease activities (*4*) and is conserved in all species examined from yeast to man (*6*, *7*). Pol $\gamma-\alpha$ belongs to the family A DNA polymerase group, characterized by conserved amino acid sequence motifs that constitute the pol and exo active sites (*8*, *9*). A third catalytic activity, 5′-deoxyribose phosphate lyase, has also recently been shown in pol γ and other family A pols (*10*−*12*). The smaller accessory subunit of pol γ, pol $\gamma-\beta$, has been cloned from *Drosophila* (*5*), frog (*13*), and man (*5*, *14*−*16*). It shares conserved protein domains with aminoacyl tRNA synthetases (aaRSs) (*13*, *17*) and has been suggested to participate in primer recognition (*17*) and demonstrated to increase the template-primer binding affinity, catalytic efficiency and processivity of the holoenzyme (*13*−*16*, *18*).

The recent development of several systems for reconstitution of animal pol γs (*13*−*16*, *18*) opens new avenues for study of structure−function relationships in this rare but critical cellular enzyme. We have developed an in vivo reconstitution approach in the baculovirus system (*18*) to produce recombinant *Drosophila* pol γ that exhibits physical and catalytic features indistinguishable from the native enzyme from *Drosophila* embryonic mitochondria (*1*). We report here an extension of this approach to evaluate subunit interactions in the *Drosophila* pol γ heterodimer.

EXPERIMENTAL PROCEDURES

Materials

Enzymes and Proteins. Native *Drosophila* pol γ fraction VI was prepared from embryonic mitochondria as described by Wernette and Kaguni (*1*); the recombinant holoenzyme and the isolated catalytic subunit were prepared from baculovirus-infected Sf9 cells as described by Wang and Kaguni (*18*). Restriction enzymes were purchased from Life Technologies and New England BioLabs. Deep Vent and *Pfu* DNA polymerases for PCR were purchased from New England BioLabs and Stratagene, respectively. Rabbit antisera raised against recombinant pol $\gamma-\alpha$ and pol $\gamma-\beta$ expressed in bacteria were prepared as described Wang et al. (*5*). The TNT kit for in vitro transcription/translation was purchased from Promega.

Nucleotides and Nucleic Acids. Unlabeled deoxy- and ribonucleotides were purchased from Pharmacia BioTech. [^{3}H]dTTP, [α-^{32}P]dATP, and [γ-^{32}P]ATP were purchased from ICN Biochemicals. Plasmid DNAs pET-11a, pET-16b, and pET-23d were purchased from Novagen. cDNAs encoding *Drosophila* pol $\gamma-\alpha$ and pol $\gamma-\beta$ were cloned previously into pET-11a and pET-16b (*4*, *5*). Baculovirus transfer vector pVL1392/1393 and linearized, modified baculovirus AcM-

† This work was supported by National Institutes of Health Grant GM45295.

* To whom correspondence should be addressed. Phone: (517) 353-6703. Fax: (517) 353-9334. E-mail: lskaguni@msu.edu.

[1] Abbreviations: pol, DNA polymerase; aaRS, aminoacyl tRNA synthetase; nt, nucleotide(s); DTT, dithiothreitol; PMSF, phenylmethanesulfonyl fluoride.

10.1021/bi010102h CCC: $20.00
Published on Web 03/22/2001

NPV DNA (BaculoGold) were purchased from PharMingen. The pol $\gamma-\alpha$ and pol γ-β cDNAs were cloned previously into pVL1392/1393 and designated as pVLGA and pVLGB, respectively (*18*). Synthetic oligodeoxynucleotides were synthesized in an Applied Biosystems model 477 oligonucleotide synthesizer.

Bacterial Strains. *Escherichia coli* XL-1 Blue [*recA1, endA1, gyrA96, thi, hsdR17, supE44, relA1, lac*, (*F′proAB, lacIqZ M15, Tn10* (tet^r)] was used for bacterial cloning. *E. coli* BL21 (λDE3) (Novagen) was used for the expression of recombinant proteins cloned in the pET vectors.

Insect Cells and Tissue Culture Medium. Sf9 (*Spodoptera frugiperda*) cells were passed from frozen stocks (*16*). TC-100 insect cell culture medium and fetal bovine serum were purchased from Life Technologies.

Chemicals. Isopropylthio-β-D-galactoside, nitro blue tetrazolium, 5-bromo-4-chloro-3-indolyl phosphate, and tryptose broth were purchased from Sigma. Sodium metabisulfite and leupeptin were purchased from the J. T. Baker Chemical Co. and the Peptide Institute (Minoh-Shi, Japan), respectively. Amphotericin, penicillin-G, streptomycin, and phenylmethanesulfonyl fluoride (PMSF) were purchased from Sigma. Nickel-nitriloacetic acid-agarose (Ni-NTA agarose) was purchased from Qiagen. [^{35}S]Methionine was purchased from ICN Biochemicals.

Methods

Plasmid Construction for Pol $\gamma-\beta$ Mutant Expression in E. coli. Four pol $\gamma-\beta$ mutants were constructed by standard PCR cloning from the pol $\gamma-\beta$ cDNA in pET-11a using the following primer pairs: pol $\gamma-\beta$(1−318), 5′-cgctggacatATGAGTCGCATACAACG-3′ and 3′-TATACGACCCGTATGGAatcctaggacc-5′; pol $\gamma-\beta$(1−262), 5′-cgctggacatATGAGTCGCATACAACG-3′ and 3′-CACCTTAACGGACACACatcctaggatc-5′; pol $\gamma-\beta$(41−355), 5′-agaccATGgAGCATTGGACACGACTACG-3′ and 3′-GCTACATGGCCTGATAAATgagctcgtg-5′; pol $\gamma-\beta$(101−355), 5′-agaccATGgctACTTGCTCTGGTCCCAC-3′ and 3′-GCTACATGGCCTGATAAATgagctcgtg-5′.

Upper case letters indicate the cDNA sequence of pol γ-β, and lower case letters indicate sequences added as linkers for cloning; restriction endonuclease cleavage sites are indicated by underscore. A typical PCR was carried out with 50−100 ng of plasmid DNA in a 50 μL reaction mixture under conditions recommended by New England BioLabs for the Deep Vent enzyme. The PCR products were gel purified, digested with the appropriate restriction endonucleases, and inserted into pET-11a or pET-16b to produce N-terminal histidine (His)-tagged fusion proteins, or pET-23d to produce C-terminal His-tagged fusion proteins. A fifth mutant, pol $\gamma-\gamma$(101−295), was prepared by digestion of the pol $\gamma-\beta$(101−355) plasmid DNA with *Nco*I and *Eco*RI and then inserted into pET-23d at its *Nco*I and *Hinc*II sites by standard recombinant DNA methods.

Bacterial Overexpression, Preparation of Cell Lysates, and Purification of His-Tagged Fusion Proteins. Recombinant plasmid-containing BL21(λDE3) cells (1 L) were grown at 37 °C with aeration in Luria broth containing 100 μg/mL ampicillin. When the optical density at 600 nm reached 0.8−1.0, isopropylthio-β-D-galactoside was added to 1 mM, and the culture was incubated for an additional 4 h. Cells were harvested by centrifugation at 5000*g* for 15 min. Cell pellets were either stored at −80 °C or were processed directly for Ni-NTA agarose affinity purification. Purification of His-tagged fusion proteins was performed by the procedure recommended by Qiagen for denaturing purification of insoluble proteins. Briefly, cell pellets were suspended in buffer B (8 M urea, 0.1 M sodium phosphate, 0.01 M Tris-HCl, pH 8.0) in a volume of 5 mL per gram of cell pellet. Cells were lysed by stirring for 1 h at room temperature. The lysate was collected by centrifugation at 10000*g* for 15 min at 4 °C, and loaded onto a 2 mL of Ni-NTA agarose column at a flow rate of 10−15 mL/h. The column was washed with 10 column volumes of buffer B, followed by 5 column volumes of buffer C (8 M urea, 0.1 M sodium phosphate, 0.01 M Tris-HCl, pH 6.3). The His-tagged fusion proteins were eluted with 300 mM imidazole in buffer C.

Protein Overlay Assays. Recombinant pol $\gamma-\beta$ proteins were expressed in *E. coli* and purified by Ni-NTA agarose affinity chromatography as described above. Samples containing 1−2 μg of pol $\gamma-\beta$ protein were subjected to 12% SDS−PAGE and transferred to nitrocellulose membranes (PROTRAN, Schleicher & Schuell) for 4−6 h at 200 mA in a TE Series Transphor Electrophoresis Unit (Hoefer Scientific Instruments). Prestained protein standards (New England BioLabs) were used as molecular weight markers. The nitrocellulose membranes were trimmed to a minimal size and blocked with 0.5% bovine serum albumin (Sigma) in 20 mM Tris-HCl, pH 7.5, 150 mM NaCl, and 0.05% (v/v) Tween 20 (TBST) containing 2.5 mM $MgCl_2$ and 2 mM dithiothreitol (DTT) for 45−60 min at room temperature, followed by a TBST wash for 5 min. The blots were then incubated overnight at 4 °C in TBST containing 1 mM PMSF, 10 mM sodium metabisulfite, 2 μg/mL leupeptin, 2 mM DTT, and [^{35}S]methionine-labeled protein probes that were prepared using the TNT kit as described by the manufacturer (Promega). The blots were washed five times with TBST for 10−15 min at room temperature and were then dried and exposed to a PhosphorImager screen (Molecular Dynamics). The data were analyzed using the ImageQuant version 4.2a software. Quantitation involved normalizing the radioactive signals produced to the physical amount of homogeneous pol $\gamma-\beta$ proteins present on the blot as determined both by india ink staining and immunoblotting of protein electrophoresed in parallel lanes. That the stained/immunoblot signals scanned were in the linear range of detection was determined in control analyses in which several amounts of the pol $\gamma-\beta$ proteins were electrophoresed. With regard to the probes, they were labeled to similar specific activities, and equivalent amounts of total radioactivity were used. Because their actual specific activities, in terms of fraction of probe capable of interaction, cannot be determined readily, quantitation of the data was performed by comparing the fraction interacting, i.e., radioactive signal, for each pol $\gamma-\beta$ mutant on individual blots to the wild-type pol $\gamma-\beta$ control on the same blot; by this method, blots in which different probes were used were not compared directly.

Construction of Recombinant Baculoviruses. Baculovirus transfer vectors carrying various pol $\gamma-\alpha$ and pol $\gamma-\beta$ mutants were prepared by QuickChange mutagenesis with *Pfu* DNA polymerase (Stratagene) according to the manufacturer's recommendations. A typical PCR was carried out

in a 50 μL reaction mixture with 50 ng of DNA template (pVLGA or pVLGB) and 2 units of *Pfu* DNA polymerase. A specific primer pair was used for each mutant as follows.

Primer pairs for pol γ-α mutants were pol γ-$\alpha\Delta$(483−533), 5′-GGAGATTAAGGATTCTGGA∧CTAGAGGATGACGAAGAGCCG-3′ and 3′-CCTCTAATTCCTAAGACCT∧GATCTCCTACTGCTTCTCGGC-5′; pol γ-$\alpha\Delta$(483−674), 5′-GGAGATTAAGGATTCTGGA∧AATGGACCTTCCTTTCGAGTG-3′ and 3′-CCTCTAATTCCTAAGACCT∧TTACCTGGAAGGAAAGCTCAC-5′; pol γ-$\alpha\Delta$(536−581), 5′-GGGAAGATGAAATTCTAGAG∧TTTCGCAGCGATTCAGAAGG-3′ and 3′-CCCTTCTACTTTAAGATCTC∧AAAGCGTCGCTAAGTCTTCC-5′; pol γ-$\alpha\Delta$(413−470), 5′-CCAACTGGGAGCGGTACATA∧AAGCCTCTTCCTACAGTGG-3′ and 3′-GGTTGACCCTCGCCATGTAT∧TTCGGAGAAGGATGTCACC-5′; pol γ-$\alpha\Delta$(27−126), 5′-GCAGTAGCGTGAAGATCTTT∧ATTGCCAAGGAACAAGTGCAGC-3′ and 3′-CGTCATCGCACTTCTAGAAA∧TAACGGTTCCTTGTTCACGTCG-5′; pol γ-$\alpha\Delta$(27−492), 5′-GCAGTAGCGTGAAGATCTTT∧AAGTTTCAGCACCTCTATGAT-3′ and 3′-CGTCATCGCACTTCTAGAAA∧TTCAAAGTCGTGGAGATACTA-5′; pol γ-$\alpha\Delta$(128−404), 5′-TTGAAGAGCACTTCCACAACATT-∧AATTCCAACTGGGAGCGG-3′ and 3′-AACTTCTCGTGAAGGTGTTGTAA∧TTAAGGTTGACCCTCGCC-5′; and pol γ-$\alpha\Delta$(27−742)- 5′, GCAGTAGCGTGAAGATCTTT∧AATGAATTCACTGGCGAAAAGTGCC-3′ and 3′-CGTCATCGCACTTCTAGAAA∧TTACTTAAGTGACCGCTTTTCACGG-5′.

Primer pairs for pol γ-β mutants were pol γ-$\beta\Delta$(213−246), 5′-CCGATGCGCGAACGGGTGAA∧CTCTTACACCGCGTTCTG-3′ and 3′-GGCTACGCGCTTGCCCACTT∧GAGAATGTGGCGCAAGAC-5′; pol γ-$\beta\Delta$(37−242), 5′-CATGGAAGGGAATACGCCAAA∧TCGCAATCCCTGCTCTTACAC-3′ and 3′-GTACCTTCCCTTATGCGGTTT∧AGCGTTAGGGACGAGAATGTG-5′; pol γ-$\beta\Delta$(61−104), 5′-GCCACGAGAGAACCCATAAAT∧CCCACTAGCCATTCCCTATTTG-3′ and 3′-CGGTGCTCTCTTGGGTATTTA∧GGGTGATCGGTAAGGGATAAAC-5′; pol γ-$\beta\Delta$(129−160), 5′-CGGACTTCCTAGTGGAACCA∧TGCGATTTGGCTGAGGATCTC-3′ and 3′-GCCTGAAGGATCACCTTGGT∧ACGCTAAACCGACTCCTAGAG-5′; pol γ-$\beta\Delta$(264−274), 5′-TGTGGAATTGCCTGTGTGGAA∧CTTTGTCAGCATCTGAAACAT-3′ and 3′-ACACCTTAACGGACACACCTT∧GAAACAGTCGTAGACTTTGTA-5′; pol γ-$\beta\Delta$(327−346), 5′-ACACTTGTTATAAACGAGCAA∧CACATAAGCGATGTACCGGAC-3′ and 3′-TGTGAACAATATTTGCTCGTT∧GTGTATTCGCTACATGGCCTG-5′; pol γ−β(1−349), 5′-CCATACACATAAGCtGATGTACCGGACT-3′ and 3′-GGTATGTGTATTCGaCTACATGGCCTGA-5′; pol γ−β L52P, 5′-CCTTGGCTGCGCACC**C**(T)GGGCGCCACGAG-3′ and 3′-GGAACCGACGCGTGG**G**(A)CCCGCGGTGCTC-5′; and pol γ−β L38VL45V, 5′-CCAAACTG**G**(T)TGCAACAGCATTGGACACGA**G**(C)TACGTCCC-3′ and 3′-GGTTTGAC**C**(A)ACGTTGTCGTAACCTGTGCT**C**(G)ATGCAGGG-5′.

"∧" indicates the position of deleted nucleotide residues, bold letters indicate nucleotides that replace those in parentheses, and lower case letters indicate nucleotide insertions.

The DNA template was first denatured at 95 °C for 45 s, followed by 20−25 three-step cycles of 95 °C for 45 s, 50 °C for 1 min, and 68 °C for 2 min/kbp DNA template. The reaction mixture was then digested with 10 units of *Dpn*I for 2 h at 37 °C to eliminate the methylated parental DNA template. A 2 μL aliquot was used for transformation of competent *E. coli* XL-1 Blue cells by electroporation using an *E. coli* Pulser (Bio-Rad). DNA sequence analysis of the various plasmid constructs was performed to confirm their structure and sequence integrity. Mutant pol γ−β(1−200) was cloned by standard recombinant DNA methods into pVL1392 at its *Pst*I and *Bam*HI restriction sites, using the PCR product of the primer pair 5′-gatctgcagATGAGTCGCATACAACGA-3′ and 3′-CACCTGCTGTTTCTGAtcctaggacc-5′.

Transfer vectors encoding the pol γ-α and pol γ-β mutants were purified and baculoviruses prepared as described by Wang and Kaguni (*18*). Viral stocks were prepared by amplification from single plaques.

Monitoring Reconstitution of Pol γ by Phosphocellulose Chromatography. Soluble extracts from ~6 × 10^7 Sf9 cells coinfected with pairs of pol γ−α and pol γ−β recombinant baculoviruses were prepared and fractionated by phosphocellulose chromatography as described by Wang and Kaguni (*18*) with some modifications. Levels of protein expression were compared at several multiplicities of infection, and under these conditions that employ a multiplicity of infection of 5, expression levels were comparable for all of the constructs.

The homogenization buffer (5 mL) contained 15 mM HEPES pH 8.0, 2 mM $CaCl_2$, 5 mM KCl, 0.5 mM EDTA, 280 mM sucrose, 1 mM PMSF, 0.5 mM DTT, 10 mM sodium metabisulfite, and 2 μg/mL leupeptin. Fraction I was adjusted to an ionic equivalent of 60 mM potassium phosphate and loaded onto a phosphocellulose column (2.5 mL) equilibrated with 60 mM potassium phosphate buffer (60 mM potassium phosphate, pH 7.6, 10% glycerol, 2 mM EDTA, 0.5 mM DTT, 1 mM PMSF, 10 mM sodium metabisulfite, and 2 μg/mL leupeptin) at a flow rate of 2.5 mL/h. The column was washed with 5 vol of 60 mM potassium phosphate buffer at a flow rate of 5 mL/h. Bound proteins were eluted with 5 volumes of 300 mM potassium phosphate buffer at a flow rate of 5 mL/h.

Gel Filtration Chromatography. Aliquots of pooled peak fractions (0.2−0.4 mL) from phosphocellulose chromatography were applied to a Sephacryl S-200 Superfine (Pharmacia) gel filtration column (~1 cm × 80 cm). The column was equilibrated and run in buffer containing 50 mM sodium phosphate, pH 7.5, 10% glycerol, 1 mM PMSF, 0.5 mM DTT, 10 mM sodium metabisulfite, 2 μg/mL leupeptin. The column was calibrated with a mixture of Dextran Blue 2000, yeast alcohol dehydrogenase, phosphorylase b, bovine serum albumin, carbonic anhydrase, and cytochrome *c* (100−200 μg each). Fractions were eluted collected in a volume of 0.2−0.3 mL.

Other Methods. Chromatographic steps for protein purification were as described by Wang and Kaguni (*18*). UV cross-linking was performed as described by Olson et al. (*3*) with specific modifications as indicated in the legend to Figure 5. The substrate used is depicted in Figure 5 and consists of an 142 nt RNA (5′-GGGCGAAUUGGGUACCGGAAUUGCCUUUGCCAAACUUUUAGAAGUAAAGUAUGCUUAUGGAAUUAUGGAUUUUUUGUUGUUUUUGUUGUUUGUUUAGAUCGAAUUCCUGCAGCCC-

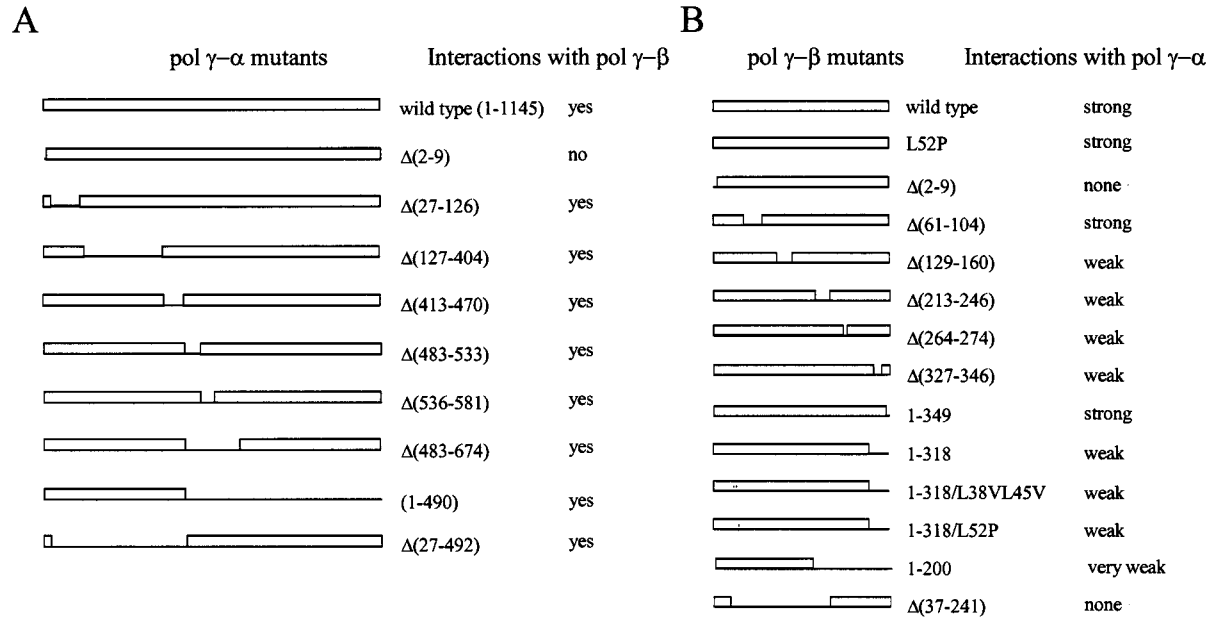

FIGURE 1: Baculovirus constructs of the catalytic and accessory subunits of *Drosophila* pol γ and summary of in vivo holoenzyme reconstitution. The complete coding sequences of the catalytic (pol γ−α, 1145 amino acid residues) and accessory (pol γ−β, 361 amino acid residues) subunits of *Drosophila* pol γ were subcloned from their respective bacterial expression plasmids into the baculovirus transfer vector pVL1392/1393, and recombinant baculoviruses were prepared (*18*). Mutant constructs as indicated were prepared by deletion (and/or site-directed) mutagenesis. Open boxes indicate the sequences present and solid lines indicate those that are deleted relative to the wild-type. In vivo reconstitution of mutant subunits with their respective wild-type partners was monitored by phosphocellulose chromatography as described in the Experimental Procedures. A summary of the subunit interaction data is shown.

GGGGGAUCCACUAGUUCUAGAGCGGCC-3′) that was synthesized by in vitro transcription with T7 RNA polymerase (*19*), 5′-end labeled with T7 polynucleotide kinase, and annealed to a 27 nt deoxynucleotide (5′-ATATATAA-TATTGGCCGCTCTAGAACT-3′). Protein concentrations were determined by the method of Bradford (*20*) with bovine serum albumin as the standard. Gel electrophoresis and protein transfer and immunoblotting were performed as described by Wang and Kaguni (*18*).

RESULTS

The Accessory Subunit Interacts through Multiple Sites with the Catalytic Subunit in Drosophila pol γ. To elucidate structure−function relationships in the *Drosophila* pol γ holoenzyme, we undertook a comprehensive study of subunit interactions, by production of altered forms of the two subunits and assessment of enzyme reconstitution in the baculovirus system. We constructed nine variants of the catalytic subunit and 13 of the accessory subunit by deletion mutagenesis, and then prepared recombinant baculoviruses (Figure 1). We tested subunit interaction by phosphocellulose chromatography of presumptive reconstituted holoenzyme forms (see Experimental Procedures). Under the experimental conditions used, both the holoenzyme and the catalytic subunit bind tightly to phosphocellulose and are eluted at ∼200 and 300 mM potassium phosphate, respectively. In contrast, we found that the accessory subunit does not bind to phosphocellulose at all in the absence of holoenzyme reconstitution.

To investigate interacting regions in the accessory subunit, β-subunit variants were coexpressed with the wild-type catalytic subunit (with or without a C-terminal hexahistidine tag) in Sf9 cells. The assembly of altered holoenzyme was monitored by phosphocellulose chromatography, and interaction data were confirmed by additional steps including gel filtration on Sephacryl S-200, Ni-NTA agarose, Cibacron blue agarose, or single-stranded DNA cellulose chromatography. This approach allowed us to identify two classes of altered forms of the *Drosophila* pol γ holoenzyme: those which assemble and are relatively stable and those which assemble to some extent but exhibit limited stability during the course of purification, at least in part due to salt sensitivity in chromatographic elution profiles. An example of each class is represented by the altered holoenzymes pol γ−α/βΔ(61−104) and pol γ−α/β(1−318), respectively (Figure 2). Pol γ−α/βΔ(61−104) shows strong subunit association through four purification steps: a soluble extract was fractionated on phosphocellulose followed by ammonium sulfate precipitation, and sequential chromatography on Ni-NTA agarose and Cibacron blue agarose (Figure 2A). In contrast, when an extract of pol γ−α/β(1−318)-infected Sf9 cells was fractionated on phosphocellulose, only limited coelution of the two subunits was observed (Figure 2B, left). Furthermore, while gel filtration of the peak fraction (no. 10) confirmed the formation of a complex (fractions 19−23, Figure 2B, right), a relatively large portion of free catalytic subunit was also observed (fractions 25−29), indicating subunit dissociation during chromatography. The relatively weak subunit interaction in pol γ−α/β(1−318) was explored further in a triple infection analysis with baculoviruses encoding pol γ−α, wild-type pol γ−β, and pol γ−β(1−318) (Figure 2C). In the presence of a 2-fold excess of wild-type pol γ−β over pol γ−β(1−318), only the wild-type β subunit coeluted with pol γ−α upon phosphocellulose chromatography, suggesting the interaction between pol γ−α and the mutant pol γ−β-(1−318) polypeptide is reduced to less than 30%. This experiment also shows that the elution profile upon phosphocellulose chromatography can be used to monitor directly

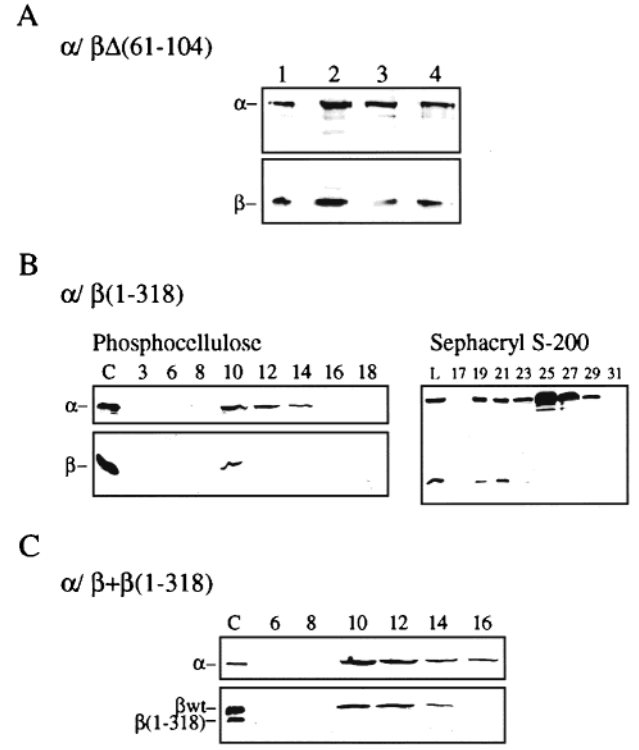

FIGURE 2: Baculovirus reconstitution and purification of β-subunit mutant pol γ. (A) pol $\gamma-\alpha/\beta(\Delta 61-104)$ A soluble extract prepared from Sf9 cells co-infected with recombinant baculoviruses expressing the wild-type α and mutant $\beta(\Delta 61-104)$ subunits was chromatographed on phosphocellulose as described by Wang and Kaguni (*18*), and peak fractions eluting at ~200 mM KPO_4 were pooled and fractionated with ammonium sulfate at 55% saturation. The precipitate was applied to a Ni-NTA agarose column and peak fractions eluting at ~500 mM imidazole were pooled and applied to a Cibacron blue agarose column (*36*). Peak fractions eluting in ~0.75 M NaSCN were pooled. Column eluates were analyzed in a 10% SDS−polyacrylamide gel, and the recombinant polypeptides were detected by immunoblotting with subunit-specific antisera. Lane 1, soluble extract; lane 2, phosphocellulose pool precipitated with ammonium sulfate; lane 3, Ni-NTA agarose pool; lane 4, blue agarose pool. (B) pol $\gamma-\alpha/\beta(1-318)$ (left) a soluble extract was chromatographed on phosphocellulose. The numbered elution fractions were analyzed by SDS−PAGE and immunoblotting. "C" indicates a total cell extract electrophoresed as a control. (Right) The peak fraction (no. 10) eluting from phosphocellulose at ~200 mM KPO_4 was subjected to gel filtration on Sephacryl S-200. Numbered elution fractions were analyzed as above. "L" indicates the load fraction. (C) A soluble extract prepared from Sf9 cells co-infected with recombinant baculoviruses expressing wild-type pol $\gamma-\alpha$, wild-type pol $\gamma-\beta$, and pol $\gamma-\beta(1-318)$ was chromatographed on phosphocellulose, and the numbered elution fractions were analyzed by SDS−PAGE and immunoblotting. "C" indicates a total cell extract electrophoresed as a control.

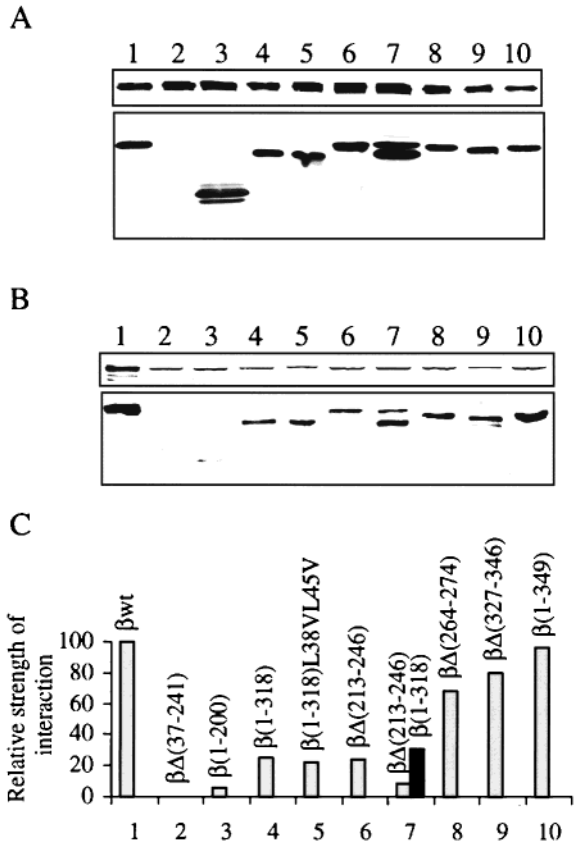

FIGURE 3: Reconstitution of altered holoenzyme forms of *Drosophila* pol γ in baculovirus-infected Sf9 cells. Sf9 cells were infected at a multiplicity of infection of 5 with recombinant baculoviruses expressing the wild-type α and various mutant β subunits. (A) The expression level of individual recombinant proteins was monitored by 10% SDS−PAGE and immunoblotting of total cell extracts with subunit-specific antisera. The expression level of each of the constructs (with lane numbers identified in panel C) was found to be approximately the same, except for $\beta\Delta(37-241)$ which was expressed very poorly. (B) Soluble cytoplasmic fractions were chromatographed on phosphocellulose as described in the Experimental Procedures. The peak fractions eluting at ~200 mM KPO_4 were pooled and analyzed by 10% SDS−PAGE and immunoblotting. (C) Graphic representation of the interaction data. Relative strengths of interaction were determined by densitometric scanning of the blot in panel B. The data are represented as percentages of the interaction of wild-type pol $\gamma-\beta$ (lane 1), after normalization of the relative intensities of the pol γ-α bands. Figure 3 presents a composite analysis of data derived from several independent co-infections with each virus pair. In control analyses, several aliquots of each of the cell extracts (A) and phosphocellulose eluates (B) were immunoblotted to ensure that densitometric scanning was in the linear range.

the interactions between pol $\gamma-\alpha$ and individual pol $\gamma-\beta$ mutants that are coexpressed in Sf9 cells. Thus, if the expression levels of pol $\gamma-\alpha$ and the pol $\gamma-\beta$ variants are similar, the relative amount of the individual pol $\gamma-\beta$ variants in peak fractions coeluting with pol $\gamma-\alpha$ will represent the relative strength of subunit association.

We used this approach to analyze a panel of pol $\gamma-\beta$ mutants and in most cases, the expression level of the recombinant protein pairs was very similar, except for the mutant pol γ-$\beta\Delta(37-241)$ (Figure 3A). Immunoblotting of peak fractions from phosphocellulose chromatography shows variable levels of the pol $\gamma-\beta$ mutants in the presence of similar levels of pol $\gamma-\alpha$, indicating their differing relative affinities for interaction with pol $\gamma-\alpha$ (Figure 3B). Mutant pol γ-$\beta\Delta(37-242)$ (lane 2, Figure 3B) was likely not observed in the elution fractions because of its reproducibly very low level of expression (lane 2, Figure 3A). Mutant pol $\gamma-\beta(1-200)$ (lane 3, Figure 3B) shows a very weak interaction (<10% of wild-type) with pol $\gamma-\alpha$. Other mutants exhibit interactions ranging from 20 to 80% as compared to wild-type pol $\gamma-\beta$, while pol $\gamma-\beta(1-349)$ (lane 10) shows the strongest interaction with pol $\gamma-\alpha$ (96%) (Figure 3C). That mutant pol $\gamma-\beta(1-318)$ retains only 20−30% of wild-type interaction with pol $\gamma-\alpha$ (lane 4) is in agreement with the estimation of <30% by the competitive interaction assay shown in Figure 2C. Results for these and other mutants tested are summarized in Figure 1. Mutant

$\beta\Delta(2-9)$, with the putative mitochondrial targeting sequence interrupted, shows no interaction with the catalytic subunit, confirming the previous results of Wang and Kaguni (*18*) that protein sorting is important for in vivo subunit interactions. The very weak interaction between pol $\gamma-\beta(1-200)$ and the catalytic subunit indicates that the deleted region (residues 201−361) is important for subunit interactions, and that the region of residues 1−200 can support only limited interaction. Furthermore, whereas pol γ-$\beta\Delta(129-160)$ shows reduced subunit interaction, both pol γ-$\beta\Delta(61-104)$ and pol $\gamma-\beta(1-349)$ retain strong interaction with pol $\gamma-\alpha$. These results suggest that the interaction motifs are localized mainly within residues 129−349 of the accessory subunit. Within this region of 221 amino acids, deletions such as $\Delta(213-246)$, $\Delta(264-274)$, $\Delta(327-346)$, and $\Delta(319-361)$ [which is equivalent to $\beta(1-318)$] show various reductions in subunit interaction, indicating that multiple sites are involved in subunit−subunit interaction in the *Drosophila* pol γ heterodimer.

To test if the putative leucine zipper (Lx6Lx6Lx6I) at the position of residues 38−59 in the accessory subunit is involved in subunit-subunit interaction, several β mutants [pol $\gamma-\beta$ L52P, pol $\gamma-\beta(1-318)$/L52P, and pol $\gamma-\beta(1-318)$/L38VL45V] containing proline or valine substitutions of leucine residues were analyzed. None of these substitution mutations showed significant effects on holoenzyme reconstitution (Figure 1), indicating that the leucine zipper motif plays no apparent role in subunit-subunit interaction in the *Drosophila* pol γ complex.

The Accessory Subunit of Drosophila pol γ May Consist of Three Domains with Different Functions. The above data argue that the accessory subunit interacts with the catalytic subunit through several contact sites located mainly in the region including amino acid residues 129−349. In contrast, the N-terminal region (aa1−128) in its entirety may not be important for subunit interactions, because a deletion of 45 amino acid residues in the middle of this region in mutant $\beta\Delta(61-104)$ did not affect significantly subunit interaction (Figure 2A). Instead, we would propose that the N-terminal region forms an independent domain, designated the N domain. The C-terminal region (aa254−361) shares amino acid sequence homology (~30% identity) with the anticodon binding domain of class IIa aminoacyl-tRNA synthetases, and we predicted it to fold similarly to provide the accessory subunit with the property of binding to specialized RNA primers in mtDNA replication (*17*). The intermediate region (aa129−253) may form a third domain, designated the M domain.

To evaluate the possibility that the assigned domains form independent structures, the same fold recognition analysis (*21*) used for development of the C-terminal structural model was applied independently to the presumptive N and M domains of pol γ-β. We found that the fold of the N region resembles the structure of MarA, a member of the AraC transcriptional activator class with a helix-loop-helix DNA binding motif (*22*; Z score of 5.6, just above the threshold value of 5.0 ± 1.0). The significance of the helix-loop-helix motif spanning amino acid residues 32−85 in the accessory subunit is not clear at present. However, biochemical analysis of the pol $\gamma-\alpha/\beta\Delta(61-104)$ reconstituted holoenzyme suggests roles for the N region in substrate DNA binding and in the function of the accessory protein to increase the catalytic efficiency of the holoenzyme. We examined the DNA polymerase activity of the highly purified Fraction IV enzyme (Figure 2A), and found that it exhibits an ~10-fold reduced specific activity on DNase I-activated calf thymus DNA as compared to native pol γ. Furthermore,whereas the pol $\gamma-\alpha/\beta\Delta(61-104)$ holoenzyme exhibits the general chromatographic properties of native pol γ (Figure 2A), we found that it binds single-stranded DNA cellulose poorly, eluting at ~150 mM KCl as compared to 400 mM KCl for native pol γ.

According to the structure-based sequence alignment in the fold recognition analysis, the M region of pol $\gamma-\beta$ shows significant sequence homology (30% identity over 102 amino acid residues) with the RNase H domain of the reverse transcriptase (RT) of human immunodeficiency virus (HIV), although the Z score is slightly below the threshold value (data not shown). Nonetheless, their sequence homology is comparable to those observed among known RNase H homologues. For example, previous structure-based sequence alignments showed that *E. coli* RNase H shares 28% amino acid sequence identity with a yeast RNase H enzyme, 27% with RNase H of Moloney murine leukemia virus, 19% with RNase H of Rous sarcoma virus, and 24% with the RNase H domain of HIV RT (*23*). Sequence analysis performed by Gap alignment in the GCG program shows that the M region of the accessory subunit shares 27% amino acid sequence identity (38% similarity) over 130 amino acid residues with the entire RNase H domain of HIV RT (Figure 4). Interestingly, three acidic amino acid residues (shadowed in Figure 4) that are important for *E. coli* RNase H activity (*24*) are conserved in HIV RT and are either conserved or replaced by similar residues in the M region of pol $\gamma-\beta$. In a standard RNase H assay using poly(dA): oligo(rA) (*25*), we were unable to demonstrate RNase H activity in *Drosophila* pol γ (data not shown). However, the RNase H-like M region could be involved in the proposed RNA primer binding function of the accessory subunit.

Our structural model of the C-terminal region of pol $\gamma-\beta$ predicted RNA binding as in aaRSs (*17*), and a role in primer recognition as in the γ complex of *E. coli* pol III holoenzyme (*26*−*28*). We employed a UV cross-linking analysis to obtain biochemical evidence that the β subunit in native *Drosophila* pol γ binds RNA (Figure 5). We designed a model template-primer that contains a 142 nt radiolabeled RNA primer with stable intra-strand base pairing, annealed over 15 nt to a 27 nt template DNA strand (Figure 5, left). UV cross-linking results in the identification of a pol $\gamma-\beta$: template-primer complex by SDS−PAGE and autoradiography (Figure 5, right). Notably, cross-linking of the catalytic subunit was not observed. We extended this result to evaluate binding of pol $\gamma-\beta$ to the RNA alone and found that the template DNA strand was not required (data not shown). Nonetheless, with the assembled template-primer, both β subunit cross-linking and RNA primer extension can be observed when dATP (the next required nucleotide) is added to the reaction (Figure 5, right).

The critical role of the conserved C-terminus of the accessory protein in *Drosophila* pol γ function was established by examining the DNA polymerase activity of the reconstituted and partially purified pol $\gamma-\alpha/\beta(1-318)$ in comparison with the native reconstituted holoenzyme and catalytic subunit purified previously (*18*). Using the standard

```
                    β1          β2          β3          α1
E. coli RNase H   1 ..MLKQVEIFTDGSCLGNPGPGGYGAILRYRGREKTFSAG..YTRTTN....N 45
HIV RT RNase H  432 EPIVGAETFYVDGAANRETKLGKAGYVTNK...GRQKVVP..LTNTTN....Q 475
pol γ–β         127 EPHRALEHFY.NM..QRESKIWWMRLSSNP...SRYRIVPCDLAEDLNPNDYQ 173

                    α1          β4      α2      α3
E. coli RNase H    46 RMELMAAI.....VALEALKEHCEVILSTDSQYVRQGITQWIHNWKKR(10)K 96
HIV RT RNase H  476 KTELQAIY.....LALQDSG..LEVNIVTDSQYALGIIQAQ.......PDKSE 519
pol γ–β         174 AIDIRTSYGDAGEVAVEQLS. L.VRIVDDKDFRL.............PDART 216

                    α4          β5          α5
E. coli RNase H    97 NVDLWQ.RLDAALGQH.QIKWEWVKGHAGHPENERCDELARAAAMNPTLEDTG 150
HIV RT RNase H  520 .SELVN.QIIEQLIKKEKVYLAWVPAHKGIGGNEQVDKLVSAGIRKIL       560
pol γ–β         217 .GETVQPTVIRSVIELETTTCALLLDGCDHGRDSQSLLLHRVLA          253
```

FIGURE 4: Sequence homology between the M region of the accessory subunit of *Drosophila* pol γ, the RNase H domain of HIV-1 reverse transcriptase and *E. coli* RNase H. A sequence alignment of the M region of the accessory subunit (pol $\gamma-\beta$) of *Drosophila* pol γ and the RNase H domain of HIV-1 reverse transcriptase was produced by *Gap* alignment in the GCG program package. The sequence of *E. coli* RNase H was added based on its structural-based alignment with HIV RT RNase H (*37*). (|) Identical amino acid residues; (:) highly similar amino acid residues; and (.) similar amino acid residues. The bars above the alignment indicate the secondary structural elements in *E. coli* RNase H (*23*). The M region of *Drosophila* pol $\gamma-\beta$ and the RNase H domain of HIV RT share 26.6% identity and 38.4% similarity over the aligned region. Three acidic residues important for *E. coli* RNase H activity are shadowed.

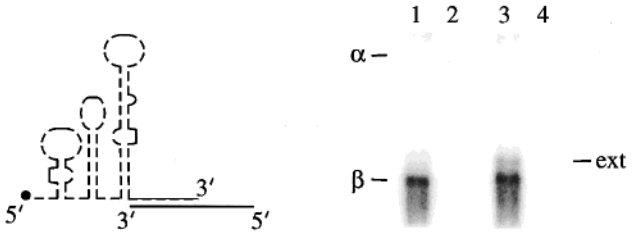

FIGURE 5: RNA binding by the accessory subunit measured by UV cross-linking of *Drosophila* pol γ to template-primer DNA. (Left) Schematic representation of the template-primer used for UV cross-linking analysis. The template-primer consists of a [^{32}P]RNA (142 nt) annealed over 15 nt to a 27 nt template DNA strand (see Experimental Procedures). (Right) Near-homogeneous recombinant pol γ (10 fmol) was incubated with template-primer (20 fmol) for 15 min at 30 °C under standard DNA polymerase assay conditions in the absence (lanes 1 and 2) or presence (lanes 3 and 4) of dATP. The reaction mixture was UV irradiated for 15 min on ice. Proteins were analyzed by 10% SDS−PAGE and autoradiography to monitor RNA cross-linking. Lanes 2 and 4 represent no enzyme controls. *ext* marks the position of the extended RNA primer (see text).

assay on DNase I-activated calf thymus DNA in the presence of aphidicolin and at various KCl concentrations, we found that the reconstituted pol $\gamma-\alpha/\beta(1-318)$ enzyme exhibits the catalytic properties of the isolated catalytic core, with a specific activity of ~2% of the native holoenzyme and a clear salt-sensitivity. This data indicates that the function of the β subunit to increase the catalytic efficiency of the core is lost by deletion of its C-terminus.

Contacts between Amino Acid Residues 1−490 of the Catalytic Subunit and the C and M Regions of the Accessory Subunit Provide the Dominant Force of Subunit Interactions in Drosophila pol γ. Reconstitution of altered holoenzymes with nine variants of the catalytic subunit and the wild-type accessory subunit in Sf9 cells was monitored by phosphocellulose chromatography as described earlier, and the results are summarized in Figure 1. All but one of the catalytic subunit mutants, including those with deletions of several hundred amino acid residues spanning the entire polypeptide, were found to interact with the accessory subunit. The exception was mutant pol γ-$\alpha\Delta(2-9)$ which has the mitochondrial target sequence deleted. These results argue that the catalytic subunit interacts with the accessory subunit through multiple contacts. The relative strength of individual pol $\gamma-\alpha$ mutant interactions cannot been tested directly by in vivo reconstitution because the elution profiles of the mutant polypeptides overlapped those of the reconstituted holoenzyme upon phosphocellulose chromatography.

On the basis of sequence comparison with the Klenow fragment of *E. coli* DNA pol I, the catalytic subunit of *Drosophila* pol γ can be divided approximately into three regions: the exonuclease (exo) region (aa1−430), the spacer region (aa431−750), and the DNA polymerase (pol) region (aa751−1145). Several mutants with deletions in the spacer region were investigated to test if this region is important for subunit interactions, because the corresponding part in T7 DNA polymerase provides the motif for interaction with thioredoxin. We found that the putative leucine zipper at position 483−533 within the spacer and the surrounding residues are not essential for subunit interactions: mutants pol γ-$\alpha\Delta(483-533)$, $\Delta(413-470)$, $\Delta(536-581)$, and Δ-$(483-674)$ all interact with pol $\gamma-\beta$ (Figures 1 and 6). Notably, residues 1−419 at the N-terminus of pol $\gamma-\alpha$ are sufficient to allow complex formation with pol $\gamma-\beta$. Furthermore, mutant pol γ-$\alpha\Delta(27-492)$ also forms a complex with pol $\gamma-\beta$. The interactions of pol $\gamma-\beta$ with pol $\gamma-\alpha(1-490)$ and pol γ-$\alpha\Delta(27-492)$ were investigated further (see below).

On the basis of the results described in the previous section, we have localized the interaction regions in the accessory subunit to the putative M and C domains. To understand how the presumptive domains of pol $\gamma-\alpha$ interact with those in pol $\gamma-\beta$, we monitored by phosphocellulose chromatography the reconstitution of three mutant catalytic-subunit polypeptides with the wild-type and two mutant accessory subunit proteins upon pairwise expression in Sf9

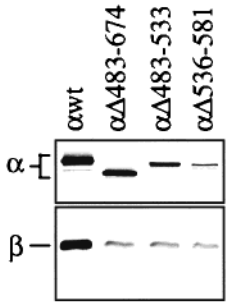

FIGURE 6: Role of the spacer region of the catalytic subunit in pol γ subunit interactions. The spacer region mutants pol γ−αΔ(483−674), pol γ−αΔ(483−533), and pol γ−αΔ(536−581) were examined for interaction with wild-type pol γ−β by pairwise co-infections in Sf9 cells and phosphocellulose chromatography, followed by SDS−PAGE and immunoblotting as described in the legend to Figure 3.

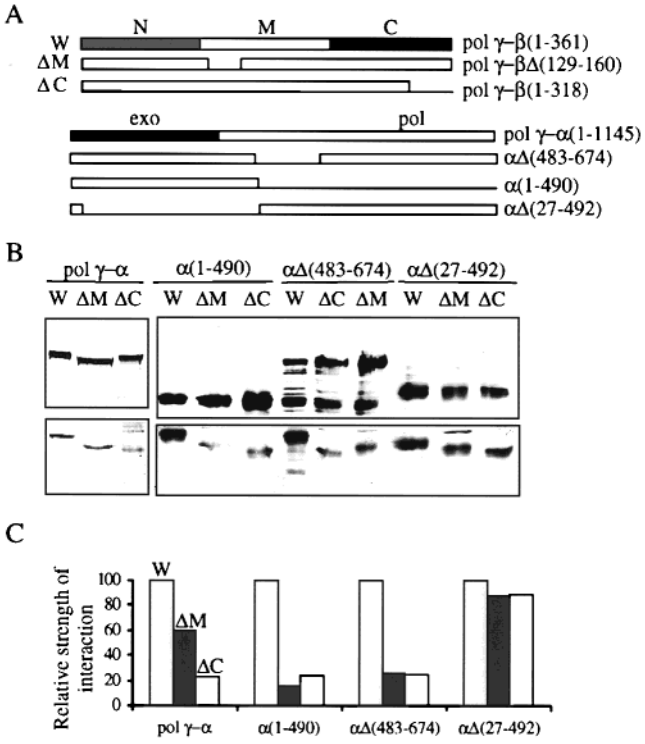

FIGURE 7: Regional interactions between the catalytic and accessory subunits of *Drosophila* pol γ measured by holoenzyme reconstitution in Sf9 cells. Recombinant pol γ−β (W), pol γ-βΔ129−160 (ΔM), and pol γ−β1−318 (ΔC) were examined for interaction with pol γ−α, pol γ−α1−490, pol γ−αΔ483−674, and pol γ−αΔ27−492 by pairwise co-infections in Sf9 cells and phosphocellulose chromatography, followed by SDS−PAGE and immunoblotting as described in the legend to Figure 3. (A) Schematic representation of the pol γ−α and pol γ−β constructs used. Boxes indicate the sequences present and solid lines indicate those that are deleted relative to the wild-type subunits. (B) Immunoblot of the SDS−polyacrylamide gel. (C) Graphic representation of the interaction data. Relative strengths of interaction were determined by densitometric scanning of the blot in panel B. The data are represented as percentages of the interaction of wild-type pol γ−β (lanes "W"), after normalization of the relative intensities of the pol γ-α bands within each group.

cells (Figure 7). The β-subunit mutants pol γ-βΔ(129−160), with a deletion of 32 amino acid residues in the M region, and pol γ−β(1−318), with a deletion of 43 residues in the C region, were selected because these deletions likely disrupt the conformation of the individual region in which the deletion occurs. Therefore, we can exclude interactions with the M region and monitor only interactions with the C region in mutant βΔ(129−160) reconstituted with the pol γ−α polypeptides; similarly, we can monitor only the interactions mediated by the M region with mutant β(1−318). As controls, wild-type pol γ−α was also tested pairwise with pol γ−β (W), pol γ-βΔ(129−160) (ΔM), and pol γ−β(1−318) (ΔC). As indicated by the relative intensities of the bands for the three pol γ−β proteins (Figure 7B), pol γ-βΔ-(129−160), and pol γ−β(1−318) show weaker interaction with pol γ−α than does wild-type pol γ−β, ∼60 and 23%, respectively (Figure 7C). Similarly, the interaction between βΔ(129−161) or β(1−318) and pol γ−α(1−490) is much weaker, only about 20% of that between pol γ−α(1−490) and pol γ-β (Figure 7, panels B and C). These results indicate that the exo region and part of the spacer (aa431−490) of the catalytic subunit interact with both the C and M regions of the accessory subunit: subunit interaction was reduced 5-fold by disruption of either region in the accessory subunit. Similar results were obtained for pol γ-αΔ(483−674), which deletes most of the spacer of the catalytic subunit. The results suggest that the region of aa675−1145, which contains mainly the pol region of the catalytic subunit, may not provide additional contacts with the accessory subunit. Together our data argue that interactions between the C and M regions of pol γ−β and the region of aa1−490 of pol γ−α are the dominant force for subunit interactions. In contrast, the same mutations in the M and C regions did not show significant differences (∼10% reduction) in interaction with pol γ-αΔ(27−492). This suggests that the region of aa493−1146 (part of the spacer and the whole pol region) of the catalytic subunit might interact with residues in the N region of the accessory subunit in the absence of the exo region. Alternatively, because the pattern of pol γ-αΔ(27−492) interaction with the three pol γ-β proteins is different from their interaction with wild-type pol γ−α, it might be concluded that the deletion of residues 27−492 might change the conformation of the remainder of the catalytic subunit, and result in interactions that differ from those which occur in native *Drosophila* pol γ.

The N Region of the Accessory Subunit May Modulate Subunit Interactions through Weak Interaction with the pol Region of the Catalytic Subunit. All of the above results are based on in vivo reconstitution of altered holoenzymes. To confirm and extend the results, we examined physical interactions in vitro by protein overlay analysis (Figure 8). Various pol γ−β mutants were expressed in *E. coli* as His-tagged fusion proteins and purified by Ni-NTA agarose affinity chromatography. The recombinant proteins were then resolved by 12% SDS−PAGE and transferred to nitrocellulose membranes. After renaturation, the immobilized proteins were probed with various ^{35}S-labeled pol γ−α mutants that were prepared by in vitro transcription/translation in the rabbit reticulocyte lysate system. The membranes were washed extensively and autoradiographed. The relative intensities of the various bands resulting from interaction between an individual ^{35}S-labeled pol γ−α probe and the pol γ−β proteins on the membrane indicate the relative strengths of the interactions. Figure 8B shows that pol γ-α-(9−1146) interacts with all of the β-subunit proteins on the membrane, indicating that the deleted mitochondrial targeting sequence is not directly involved in subunit-subunit interactions, as might be misinterpreted from the in vivo reconstitu-

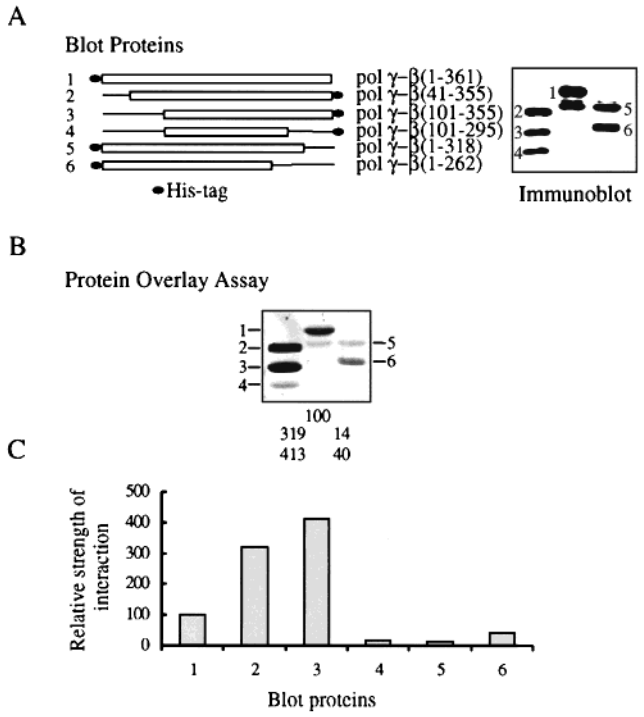

FIGURE 8: Regional interactions in *Drosophila* pol γ monitored by protein overlay blot analysis: variant forms of pol $\gamma-\beta$. His-tagged pol $\gamma-\beta$ proteins (1 μg), overexpressed and purified by Ni-NTA agarose chromatography, were fractionated by 12% SDS−PAGE and transferred to nitrocellulose membrane. The proteins were then renatured and probed with wild-type [^{35}S]pol $\gamma-\alpha$ prepared by in vitro transcription/translation (see Experimental Procedures). (A. left) Schematic representation of the pol $\gamma-\beta$ constructs used. (Right) Immunoblot analysis of the pol $\gamma-\beta$ proteins. (B) Protein overlay assay. The numbers 1−6 indicate the construct as in panel A; those under the lanes indicate the relative intensities of the mutant pol $\gamma-\beta$ bands (2−6) as compared to wild-type pol γ-β (1). (C) Graphic representation of the interaction data in panel B.

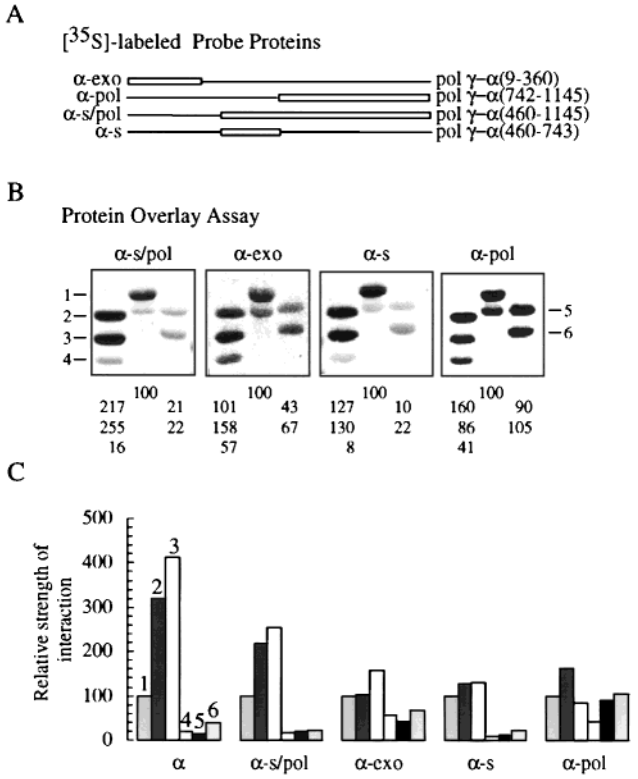

FIGURE 9: Regional interactions in *Drosophila* pol γ monitored by protein overlay blot analysis: variant forms of pol $\gamma-\alpha$. His-tagged pol $\gamma-\beta$ proteins (1 μg), overexpressed and purified by Ni-NTA agarose chromatography, were fractionated by 12% SDS−PAGE and transferred to nitrocellulose membrane. The proteins were then renatured and probed with [^{35}S]pol $\gamma-\alpha$ polypeptides prepared by in vitro transcription/translation. (A) Schematic representation of the pol $\gamma-\alpha$ constructs used. (B) Protein overlay assay. The numbers 1−6 identify the pol $\gamma-\beta$ constructs as in Figure 8A. The numbers under the lanes indicate the relative intensities of the mutant pol $\gamma-\beta$ bands (2−6) as compared to the wild-type pol γ-β (1) within each group. (C) Graphic representation of the interaction data in panel B.

tion data. The interaction of pol $\gamma-\alpha$(9−1146) with pol $\gamma-\beta$ (1−318) is only ~14% of that with pol $\gamma-\beta$, in agreement with the in vivo results shown in Figure 6, and confirming the conclusion that the C-terminal region is important for subunit-subunit interactions (Figure 8C). The weak interaction between pol $\gamma-\alpha$(9−1146) and pol $\gamma-\beta$(101−295) indicates that the M region is sufficient only for limited subunit interaction (~18% of wild-type pol $\gamma-\beta$), in agreement with the in vivo results with the deletion mutants $\beta\Delta$(129−160) and $\beta\Delta$(213−246).

In contrast, deletions of the N-terminal region of pol $\gamma-\beta$ appear to enhance protein−protein interaction because mutants pol γ-β(41−355) and pol $\gamma-\beta$(101−355) show 3- to 4-fold stronger interactions with pol γ-α(9−1146) than does the wild-type pol $\gamma-\beta$ (Figure 8C). This implies that the presence of the N region prevents the two subunits from approaching each other closely, possibly through space exclusion with parts other than the interaction regions in pol $\gamma-\alpha$. If so, these negative effects (or the enhancement by deletion) of the N-terminal region might be expected to be less significant for shorter mutant probes of pol $\gamma-\alpha$ which still retain the interaction regions. This expectation was met for probes pol $\gamma-\alpha$ (460−1146), pol $\gamma-\alpha$ (1−360), and pol $\gamma-\alpha$ (460−743) (Figure 9). The enhancement of subunit interactions provided by the deletion of residues 1−100 in pol $\gamma-\beta$ gradually decreases from 4- to 3- to 2- to 1-fold as the masses of these probes decrease. Likewise, the enhancement provided by $\beta\Delta$(1−40) decreases from 3- to 2- to 1-fold in a similar way. These results argue that the N region of pol $\gamma-\beta$ may play a role to modulate subunit−subunit interactions in *Drosophila* pol γ, either to keep the two subunits in the required orientations for productive protein−protein interaction or to maintain the complex in an active conformation. In addition, the three catalytic-subunit probes pol $\gamma-\alpha$ (460−1146), pol $\gamma-\alpha$ (1−360), and pol $\gamma-\alpha$ (460−743) all show reduced interactions with pol γ-β(1−318) and pol $\gamma-\beta$(1−262) as compared to wild-type pol $\gamma-\beta$, supporting the previous conclusion that the C region of pol $\gamma-\beta$ is important for subunit interactions.

However, pol $\gamma-\alpha$ (742−1146) shows an entirely different pattern of interactions with these pol $\gamma-\beta$ proteins. The C-terminal deletions in mutants pol $\gamma-\beta$(1−262) and pol $\gamma-\beta$(1−318) show little effect on interaction with pol $\gamma-\alpha$ (742−1146) as compared to wild-type pol γ-β, indicating that there is little physical interaction between the C region of pol $\gamma-\beta$ and the pol region of pol $\gamma-\alpha$. This is compatible with the in vivo results obtained with pol γ-$\alpha\Delta$(27−492) and pol $\gamma-\beta$(1−318). Pol $\gamma-\alpha$(742−1146) does show a weak interaction with residues 41−100 at the N-terminus of pol $\gamma-\beta$, because its interaction with pol $\gamma-\beta$(41−355) is 160% as compared 86% for pol $\gamma-\beta$(101−355). Pol $\gamma-\alpha$-

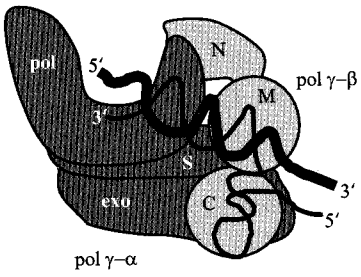

FIGURE 10: Proposed structural organization of *Drosophila* pol γ. In our working model of *Drosophila* pol γ, the catalytic subunit comprises three regions: exonuclease (exo), spacer (S), and DNA polymerase (pol), and the accessory subunit comprises N-terminal (N), middle (M), and C-terminal (C) regions as described in the text. This arrangement is based on the biochemical data presented in the text, on structural modeling (*17*, this report) and on similarities between pol γ and HIV RT (*29*, see text). The RNA-DNA substrate (thin and thick lines, respectively) is positioned to fit the proposed functions of the individual regions.

(742−1146) may also interact weakly with pol $\gamma-\beta$(101−295). However, the different pattern of pol $\gamma-\alpha$(742−1146) interactions with the pol $\gamma-\beta$ mutants as compared to those of the intact pol $\gamma-\alpha$(9−1146) polypeptide might again indicate that the deletion of residues 1−742 may change the conformation of the remainder of the polypeptide, to result in interactions different from those observed in native *Drosophila* pol γ.

DISCUSSION

Our study of subunit interactions in *Drosophila* mitochondrial DNA polymerase documents multiple interactions between the two subunits in the pol γ heterodimer. Enzyme reconstitution upon baculovirus expression of wild-type and mutant forms of both subunits shows interactions of various relative strengths occurring along the length of both polypeptides. These data are corroborated by in vitro protein overlay analyses. Combining physical and functional data, we propose a model for the overall architecture of the *Drosophila* pol γ holoenzyme that is consistent with its known (and predicted) biochemical properties (Figure 10). In the model, the catalytic and accessory subunits each consist of three regions, pol−exo−spacer in the catalytic subunit, and N−M−C in the accessory subunit. Important physical contacts occur between the exo and part of the spacer regions of the catalytic subunit and the M and C regions of the accessory subunit. Whereas the N-terminal region of the accessory subunit is not involved in direct interactions with these regions of pol γ-α in the assembled heterodimer, it may play a role in modulating assembly through weak interaction with the pol region, possibly by limiting nonproductive interactions between the pol region and the remainder of the accessory subunit. The presence of multiple contacts between the two subunits may explain our previous biochemical finding that subunit association in native *Drosophila* pol γ is so tight that separation cannot be achieved without denaturation of the enzyme (*3*). Furthermore, the extensive physical interactions between the two subunits are possibly required to keep the catalytic subunit in an active conformation, because the recombinant catalytic subunit exhibits a very low specific activity as compared with the reconstituted heterodimer (*18*). The kinetic study of recombinant human pol γ reported by Johnson and colleagues also supports this conclusion (*15*).

The proposed subunit arrangement in pol γ resembles that found in the crystal structure of HIV RT (*29*) and indeed, a number of the biochemical features of pol γ parallel those in HIV RT. HIV RT is also a heterodimer, although its p66 and p51 subunits are both encoded by the same viral *pol* gene. In native HIV RT, p66 and p51 have distinct structures (*29*), with p66 providing both the pol and RNase H activities (*30*). The p51 subunit is a proteolytic product of the p66 polypeptide that lacks the RNase H domain. Notably, although p51 does not contribute a functional active site to the HIV RT heterodimer, it is essential for the catalytic efficiency of the pol function. This parallels the critical role of the accessory subunit in the catalytic efficiency of both *Drosophila* and human pol γ (*15*, *18*). Furthermore, mitochondrial DNA polymerases from fly to man exhibit reverse transcriptase activity (*1*, *31*). Considering these features, we suggest that the pol region of pol $\gamma-\alpha$ may fold like the pol region of p66 in HIV RT. The exo region together with the spacer region would provide the corresponding regions of p51 in HIV RT, while the M region of pol $\gamma-\beta$ would correspond to the RNase H domain of p66 in HIV RT. Thus, the pol and RNase H regions are contributed by different subunits in *Drosophila* pol γ, but share a similar orientation as those in p66 of HIV RT.

HIV RT initiates minus-strand DNA synthesis with human tRNA (lys-3) whose 3′-end unfolds partially to form an 18 bp duplex with the viral RNA-primer binding site in the HIV genome (*30*). In plus-strand DNA synthesis, the RNA template is hydrolyzed by the RNase H activity of RT, leaving an oligoribonucleotide to serve as a primer. These features in HIV replication share some similarities with the initiation of mtDNA replication (*32*), and it seems plausible that *Drosophila* pol γ may employ a mechanism similar to that of RT in HIV minus-strand replication initiation as proposed by Kohlstaedt et al. (*29*). As we predicted previously in our structural model of the C-terminal region of pol $\gamma-\beta$ (*17*), we have presented biochemical evidence that the accessory subunit in *Drosophila* pol γ binds to a structured RNA, both alone and in a template−primer complex. Although it is perhaps premature to speculate that the M region in pol $\gamma-\beta$ may function as an RNase H to process the RNA transcript at the mtDNA origin into a primer with correct a 3′-OH end, our inability to date to detect RNase H activity in the *Drosophila* pol γ holoenzyme may be due to sequence and/or structural requirements such as those required by HIV RT. Minimally, our biochemical cross-linking data argue that the accessory subunit functions to position pol γ at the primer terminus for initiation of DNA strand synthesis. Notably, this proposed function of pol $\gamma-\beta$ parallels that proposed for p51 in HIV RT, in forming part of the binding sites for both the tRNA primer and the template strand (*29*).

A mutagenesis study of the accessory subunit of human pol γ showed that multiple regions of human pol $\gamma-\beta$ are required either for the activity or assembly of the human enzyme (*16*). Indeed, only those mutants of the accessory subunit that could associate with the catalytic subunit on template−primer DNA were found to stimulate the activity of the latter. Our data extend significantly those findings both to evaluate subunit interactions directly, and to map interact-

ing regions in both subunits. Although our data show some similarities with regard to critical regions in the accessory subunit, significant differences likely exist in both the structural and functional properties of *Drosophila* pol $\gamma-\beta$. Importantly, as we reported in earlier studies, only the C-terminal region of the accessory subunit is conserved among all of its homologues (*5*, *17*), and this homology extends to class IIa aaRSs in their anticodon binding domain (*13*, *17*). In class IIa aaRSs, the anticodon binding domain is also involved in the dimerization of the enzyme which is essential in most cases for their activity (reviewed in refs *33* and *34*). In this study, we have shown that the conserved C-terminus of pol $\gamma-\beta$ is important for both subunit interaction and for its biochemical function. We found that several deletions in the C-terminal region of pol $\gamma-\beta$ showed reduced levels of in vivo holoenzyme reconstitution. The nature of most of these mutations would make it difficult to distinguish the direct involvement of the deleted regions in subunit interactions from structural changes in the C-terminal region that are caused by those deletions. On the basis of our structural model (*17*), most of the mutations in pol $\gamma-\beta$ result in deletion of structural elements. An exception is mutant $\beta\Delta(264-274)$ which carries a deletion of a predicted loop in the C region. Even though mutant $\beta\Delta(264-274)$ likely retains a properly folded C-terminus, it nonetheless shows weak interaction with the catalytic subunit, suggesting that the deleted residues are involved directly in subunit association. Interestingly, a structurally corresponding region in thioredoxin (aa31−36), a predicted structural (*17*) and functional counterpart of pol $\gamma-\beta$ in the bacteriophage T7 DNA polymerase complex, is in fact involved in interaction with T7 DNA polymerase, as shown in the crystal structure (*35*). Additionally, we have shown that the reconstituted *Drosophila* pol γ mutant $\alpha/\beta(1-318)$, lacking 43 amino acid residues at the C-terminus of the accessory subunit, has a DNA polymerase specific activity comparable to that of the catalytic core alone. Thus, the conserved C-terminus of *Drosophila* pol $\gamma-\beta$ is critical for both holoenzyme structure and its function, a finding that likely extends to the vertebrate homologues.

Whereas the vertebrate pol $\gamma-\beta$s can be aligned along their entire length with Gly-RS from *T. thermophilus* (*16*), the N and M regions of the *Drosophila* accessory protein are distinct, and are more similar to other proteins in the database. Furthermore, whereas the vertebrate pol $\gamma-\beta$s share the conserved Motifs 1, 2, and 3 that are critical in aaRSs, Motif 1 is entirely lacking in *Drosophila* pol $\gamma-\beta$, and sequence-structure based alignments from fold recognition indicate that Motif 2 does not align (*17*). In contrast, we have identified here a sequence-structural homology between the M region of *Drosophila* pol $\gamma-\beta$ and the RNase H domain of HIV RT, for which we propose a function either to catalyze RNA primer processing per se, or to participate in that reaction by proper positioning of the structured RNA transcript. Finally, Lim et al. (*14*) have shown that human pol $\gamma-\beta$ binds DNA with high affinity, and both Lim et al. (*14*) and Johnson et al. (*15*) have shown that it increases the affinity of the human pol γ holoenzyme for the template-primer. We have reported here that the N-terminal region of *Drosophila* pol $\gamma-\beta$ appears to be involved in DNA binding, because the mutant reconstituted holoenzyme $\alpha/\beta\Delta(64-101)$ shows markedly reduced binding to single-stranded DNA cellulose, eluting at a position similar to that of the isolated catalytic core, and exhibiting a greatly reduced DNA polymerase specific activity that is also similar to that of pol γ-α alone. Interestingly, this region of *Drosophila* pol $\gamma-\beta$ contains a helix-loop-helix motif in a region that is not conserved among its vertebrate homologues. This renders future mutagenesis studies of both *Drosophila* and vertebrate pol $\gamma-\beta$s of significant interest in understanding the structural basis for the mechanistic features shared by all mitochondrial DNA polymerases examined to date.

ACKNOWLEDGMENT

We thank Carol Farr for her many contributions to the baculovirus expression and purification of pol γ mutants, and for her help in preparation of the figures.

NOTE ADDED IN PROOF

The recently published crystal structure of the mouse β subunit (*38*) shows it to comprise three separate domains, corroborating our physical studies of *Drosophila* β. In fact, the C-terminal domain bears a close similarity to the model of the *Drosophila* and human beta subunits proposed previously by Fan et al. (*17*).

REFERENCES

1. Wernette, C. M., and Kaguni, L. S. (1986) *J. Biol. Chem. 261*, 14764−14770.
2. Wernette, C. M., Conway, M. C., and Kaguni, L. S. (1988) *Biochemistry 27*, 6046−6054.
3. Olson, M. W., Wang, Y., Elder, R. H., and Kaguni, L. S. (1995) *J. Biol. Chem. 270*, 28932−28937.
4. Lewis, D. L., Farr, C. L., Wang, Y., Lagina, A. T., III, and Kaguni, L. S. (1996) *J. Biol. Chem. 271*, 23389−23394.
5. Wang, Y., Farr, C. L., and Kaguni, L. S. (1997) *J. Biol. Chem. 272*, 13640−13646.
6. Ye, F., Carrodeguas, J. A., and Bogenhagen, D. F. (1996) *Nucleic Acids Res. 24*, 1481−1488.
7. Lecrenier, N., Van Der Bruggen, P., and Foury, F. (1997) *Gene 185*, 147−152.
8. Ito, J., and Braithwaite, D. K. (1990) *Nucleic Acids Res. 18*, 6716.
9. Ito, J., and Braithwaite, D. K. (1991) *Nucleic Acids Res. 19*, 4045−4057.
10. Pinz, K. G., and Bogenhagen, D. F. (1998) *Mol. Cell Biol. 18*, 1257−1265.
11. Longley, M. J., Prasad, R., Srivastava, D. K., Wilson, S. H., and Copeland, W. C. (1998) *Proc. Natl. Acad. Sci. U.S.A. 95*, 12244−12248.
12. Pinz, K. G., and Bogenhagen, D. F. (2000) *J. Biol. Chem. 275*, 12509−12514.
13. Carrodeguas, J. A., Kobayashi, R., Lim, S. E., Copeland, W. C., and Bogenhagen, D. F. (1999) *Mol. Cell Biol. 19*, 4039−4046.
14. Lim, S. E., Longley, M. J., and Copeland, W. C. (1999) *J. Biol. Chem. 274*, 38197−38203.
15. Johnson, A. A., Tsai, Y., Graves, S. W., and Johnson, K. A. (2000) *Biochemistry 39*, 1702−1708.
16. Carrodeguas, J. A., and Bogenhagen, D. F. (2000) *Nucleic Acids Res. 28*, 1237−1244.
17. Fan, L., Sanschagrin, P. C., Kaguni, L. S., and Kuhn, L. A. (1999) *Proc. Natl. Acad. Sci. U.S.A. 96*, 9527−9532.
18. Wang, Y., and Kaguni, L. S. (1999) *J. Biol. Chem. 274*, 28972−28977.
19. Leung, S. S., and Koslowsky, D. J. (1999) *Nucleic Acids Res. 27*, 778−787.
20. Bradford, M. M. (1976) *Anal. Biochem. 72*, 248−254.
21. Fischer, D., and Eisenberg, D. (1996) *Protein Sci. 5*, 947−955.

22. Rhee, S., Martin, R. G., Rosner, J. L., and Davies, D. R. (1998) *Proc. Natl. Acad. Sci. U.S.A. 95*, 10413−10418.
23. Yang, W., Hendrickson, W. A., Crouch, R. J., and Satow, Y. (1990) *Sci. 249*, 1398−1405.
24. Kanaya, S., Kohara, A., Miura, Y., Sekiguchi, A., Iwai, S., Inoue, H., Ohtsuka, E., and Ikehara, M. (1990) *J. Biol. Chem. 265*, 4615−4621.
25. DiFrancesco, R. A., and Lehman, I. R. (1985) *J. Biol. Chem. 260*, 14764−14770.
26. McHenry, C. S. (1988) *Ann. Rev. Biochem. 57*, 519−550.
27. Kelman, Z., and O'Donnell, M. (1995) *Annu. Rev. Biochem. 64*, 171−200.
28. Turner, J., Hingorani, M. M., Kelman, Z., and O'Donnell, M. (1999) *EMBO J. 18*, 771−783.
29. Kohlstaedt, L. A., Wang, J., Friedman, J. M., Rice, P. A., and Steitz, T. A. (1992) *Science 256*, 1783−1790.
30. Katz, R. A., and Skalka, A. M. (1994) *Annu. Rev. Biochem. 63*, 133−173.
31. Longley, M. J., Ropp, P. A., Lim, S. E., and Copeland, W. C. (1998) *Biochemistry 37*, 10529−10539.
32. Shadel, G. S., and Clayton, D. A. (1997) *Annu. Rev. Biochem. 66*, 409−435.
33. Arnez, J. G., and Moras, D. (1997) *Trends Biochem. Sci. 22*, 211−216.
34. Cusack, S. (1997) *Curr. Opin. Struct. Biol. 7*, 881−889.
35. Doublie, S., Tabor, S., Long, A. M., Richardson, C. C., and Ellenberger, T. (1998) *Nature 391*, 251−258.
36. Farr, C. L., Wang, Y., and Kaguni, L. S. (1999) *J. Biol. Chem. 274*, 14779−14785.
37. Davies, J. F., Hostomska, Z., Hostomsky, Z., Jordan, S. R., and Matthews, D. A. (1991) *Science 252*, 88−95.
38. Carrodeguas, J. A., Theis, K., Bogenhagen, D. F., and Kisker, C. (2001) *Mol. Cell 7*, 43−45.

BI010102H